

Total fusion cross section for the ${}^9\text{Be} + {}^{28}\text{Si}$ system

J. S. Eck,* J. R. Leigh, T. R. Ophel, and P. D. Clark

Department of Nuclear Physics, Australian National University, Canberra, A.C.T. 2600, Australia

(Received 7 January 1979)

The total fusion cross sections for the system ${}^9\text{Be} + {}^{28}\text{Si}$ have been measured in the ${}^9\text{Be}$ bombarding energy range 30–60 MeV by the detection of evaporation residues in a ΔE - E ionization-chamber surface-barrier detector telescope. Although the measured ${}^9\text{Be} + {}^{28}\text{Si}$ fusion cross sections are similar to those in which a similar compound system is formed by heavy-ion ($A \geq 12$) interaction, the ratio of the measured fusion cross section to the total reaction cross section is much smaller than that observed for other systems and is attributed to the structure of ${}^9\text{Be}$ and the ease with which it breaks up into smaller fragments. This view is consistent with the anomalous ${}^9\text{Be} + {}^{28}\text{Si}$ elastic scattering results.

NUCLEAR REACTIONS ${}^9\text{Be} + {}^{28}\text{Si}$ fusion $E=30$ –60 MeV, measured fusion product angular distributions and total fusion cross sections, calculated total reaction cross section using optical model, compared fusion cross section with total reaction cross section and with fusion cross section systematics.

Elastic scattering measurements^{1–3} and analysis⁴ of the ${}^9\text{Be} + {}^{28}\text{Si}$ system in the ${}^9\text{Be}$ bombarding energy range 14–200 MeV have indicated that the interaction of ${}^9\text{Be}$ with ${}^{28}\text{Si}$ is different in some aspects from that for both lighter projectiles such as α particles, and heavier projectiles such as ${}^{12}\text{C}$ and ${}^{16}\text{O}$. In particular, the double folding model^{5,6} using a realistic nucleon-nucleon interaction, which is successful in describing the elastic α and heavy-ion scattering from such nuclei as ${}^{28}\text{Si}$ and ${}^{40}\text{Ca}$, is not successful in describing the elastic scattering for ${}^9\text{Be} + {}^{28}\text{Si}$ unless the real double folding potential is reduced by a factor ~ 0.4 . Furthermore, the optical model using either the calculated double folding potential or one of Woods-Saxon shape and classical considerations, indicates that the interaction separation for ${}^9\text{Be}$ is larger than for α and heavy-ion interactions with the same target nucleus, and that the imaginary potential necessary to describe ${}^9\text{Be}$ scattering is more diffuse than for α or heavy-ion ($A \geq 12$) scattering.^{1–3}

In order to obtain a better understanding of the ${}^9\text{Be} + {}^{28}\text{Si}$ interaction, we have measured the total fusion cross sections for ${}^9\text{Be} + {}^{28}\text{Si}$ in the ${}^9\text{Be}$ bombarding energy range 30–60 MeV. Many fusion studies conducted on similar nuclei in this mass range have investigated possible resonant structures in the fusion cross sections. The goal of the present study, on the other hand, was to investigate the average behavior of the fusion cross section in order to better understand the absorption processes for the ${}^9\text{Be} + {}^{28}\text{Si}$ system. For most systems the fusion cross section is ~ 90 –100% of the total reaction cross section at low energies, while at higher energies the fusion

cross section falls well below the total reaction cross section.⁷ These effects have been explained in terms of critical angular momenta and critical radii for fusion.⁸ In general, whether fusion takes place or not for a particular partial wave depends critically on whether the total potential (nuclear +Coulomb +centrifugal) is attractive at the critical distance for fusion. The double folding potential which is necessary to fit ${}^9\text{Be} + {}^{28}\text{Si}$ scattering must be reduced by a factor ~ 0.4 from what is calculated using the same realistic nucleon-nucleon interaction that yields a suitable folding potential fit to ${}^{12}\text{C} + {}^{28}\text{Si}$ and ${}^{16}\text{O} + {}^{28}\text{Si}$ scattering cross sections, with no reduction in the calculated potential.⁴ This reduced attractiveness of the ${}^9\text{Be} + {}^{28}\text{Si}$ potential may have an effect on the fusion cross section for this system.

The fusion cross sections for the ${}^9\text{Be} + {}^{28}\text{Si}$ system were measured using a ΔE - E ionization-chamber surface-barrier detector system⁹ by detecting the evaporation residues (the details of the measurements will be reported elsewhere). The target consisted of an 80 $\mu\text{g}/\text{cm}^2$ self-supporting foil of ${}^{28}\text{Si}$. The contamination of ${}^{16}\text{O}$ was less than 3%. The ${}^9\text{Be}$ beam was extracted from a sputter source and accelerated by the Australian National University 14UD tandem accelerator. The detector window consisted of a 30 $\mu\text{g}/\text{cm}^2$ VYNS film^{9–11} and was operated using isobutane as the counting gas at a pressure between 14–18 mm of Hg depending on the incident ${}^9\text{Be}$ energy. The data were recorded in an event mode in which each event consisted of a ΔE signal, the E signal fed through an amplifier with high gain, and the same E signal fed through an amplifier with low gain, so as to allow the elastic

scattering cross section to be measured simultaneously with the total fusion cross section. The gains of the two E signal amplifiers were scaled with energy so as to maintain the same relative threshold. The high gain energy spectrum and the low oxygen contamination in the target allowed a low energy threshold to be set. There were some events for which there was a ΔE signal and no E signal. These events can arise from either extremely low energy fusion products or from multiple scattering in the detector gas and/or window. The contribution of these events to the fusion cross section is in all cases less than or equal to $\sim 12\%$, and represents one of the largest sources of error in the reported measurements. Complete angular distributions were measured at 30, 46, and 60 MeV and are shown in Fig. 1. All residues with $Z \geq 14$ were summed to obtain the final yield. Because of the forward angle of the ΔE - E telescope, only ${}^{28}\text{Si}$ recoils from very backward scattered ${}^9\text{Be}$ projectiles, where the elastic scattering cross section is negligible, could enter the detector. At 40, 50, and 55 MeV, an angular distribution around the maximum was measured and the total fusion cross section was estimated by the simple scaling relation¹⁰

$$\sigma_{\text{TOT}}^{\text{FUS}} = 0.345 \frac{d\sigma}{d\theta}(\theta_{\text{max}}), \quad (1)$$

where

$$\frac{d\sigma^{\text{FUS}}}{d\theta} = 2\pi \sin\theta \frac{d\sigma^{\text{FUS}}}{d\Omega},$$

where all quantities are in the laboratory system. It was found from the three complete angular distributions that Eq. (1) was accurate to better than

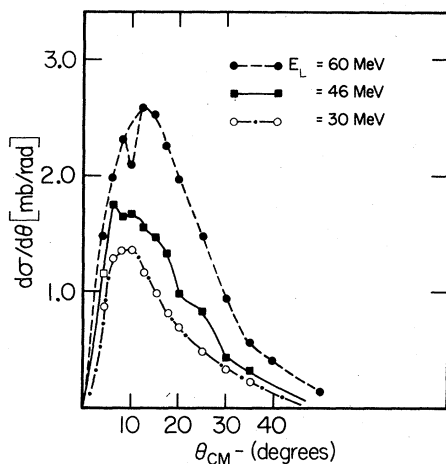


FIG. 1. Angular distributions for the evaporation residues of the ${}^9\text{Be} + {}^{28}\text{Si}$ system at $E_L = 30, 46,$ and 60 MeV. All products with $Z \geq 14$ have been summed. $d\sigma/d\theta$ is in the lab system of coordinates.

5%. The relative normalization was obtained using a fixed monitor counter, and the absolute cross sections were determined by normalizing to elastic scattering cross sections, which were measured simultaneously with the fusion measurements. Because the elastic scattering is not pure Rutherford for the angles at which the maxima occur, optical model calculations using the parameter sets which fitted the elastic scattering angular distributions were used for normalization. This procedure introduces an error of about 8% in the fusion cross section determination. The error obtained by combining the above errors and the error from counting statistics (typically 2%) leads to an error in the fusion cross section measurements of the order of 20%. This error is considerably larger than those reported in similar experiments, however, because of the lower energy of the recoiling fusion products, and the inability to normalize to Rutherford scattering in the present case; errors of this magnitude are not unexpected and are an accurate estimate of the precision of the reported measurements. The measured fusion cross sections are shown in Fig. 2 as a function of $1/E_{\text{c.m.}}$. The total fusion cross sections decrease in a fairly linear fashion with increasing $1/E_{\text{c.m.}}$ from a value of $\sigma_{\text{TOT}}^{\text{FUS}} \sim 1100$ mb at $1/E_{\text{c.m.}} = 0.022$ ($E_L = 60$ MeV) to $\sigma_{\text{TOT}}^{\text{FUS}} \sim 480$ mb at $1/E_{\text{c.m.}} = 0.044$ ($E_L = 30$ MeV). There is an indication of possible structure in the fusion cross sections at $1/E_{\text{c.m.}} = 0.033$, but more

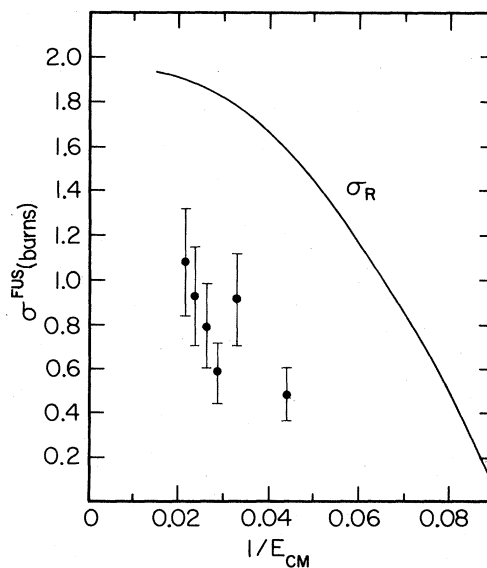


FIG. 2. Total fusion cross sections in barns for the ${}^9\text{Be} + {}^{28}\text{Si}$ system as a function of $1/E_{\text{c.m.}}$ (MeV^{-1}). The solid curve is the total reaction cross section calculated using the optical model parameters which fitted the elastic scattering angular distributions (see text).

measurements would be required before any conclusions could be drawn regarding this point. They are similar in shape but smaller in magnitude than those observed for other systems in which a similar compound system is formed. The total reaction cross section, which is calculated from the optical model with Woods-Saxon form factor using the parameter sets which fitted the elastic scattering at 45 and 60 MeV (i.e., $U=10.0$ MeV, $r_0=1.368$, $a_0=0.6067$, $W=23.4$, $r_w=1.277$, $a_w=0.6090$, and $r_c=1.35$; see Ref. 2 for details) is also shown. The calculated reaction cross sections agree within 10% to those obtained from the folding potential fits and those calculated using the energy independent potential for ${}^9\text{Be} + {}^{28}\text{Si}$ scattering of Balzer *et al.*¹ In all cases in which the optical model gives reasonable fits to the elastic scattering cross sections, the calculated reaction cross sections are insensitive to the particular parametrization utilized.

Fitting the relationship $\sigma_{\text{FUS}} = R_{\text{FUS}}^2(1 - V_B/E_{\text{c.m.}})$ to the cross section data of Fig. 2 yields values of $V_B = 22 \pm 4$ MeV and $r_{\text{FUS}} = 1.5 \pm 0.2$, where $R_{\text{FUS}} = r_{\text{FUS}}(9^{1/3} + 28^{1/3})$. The reaction radius R_R is related to the fusion radius by

$$\frac{\sigma_R}{\sigma_{\text{FUS}}} = \frac{R_R^2}{R_{\text{FUS}}^2} = \frac{r_R^2}{r_{\text{FUS}}^2}.$$

Since

$$\sigma_R/\sigma_{\text{FUS}} \approx 2.5-3$$

for the energy range investigated here, $r_R = 2.4-2.6$. The fusion radius parameter r_F , the fusion barrier V_B , and the saturation value of the fusion cross section are similar to what one would expect from fusion systematics. The total reaction cross section, however, is much greater than the measured fusion cross sections even at the lowest energies where systematics¹¹ based on studies of such systems as ${}^{12}\text{C} + {}^{27}\text{Al}$, ${}^{12}\text{C} + {}^{24}\text{Mg}$, ${}^{16}\text{O} + {}^{27}\text{Al}$, etc., would predict that $\sigma_R \approx \sigma_{\text{FUS}}$ up to values of $1/E_{\text{c.m.}} \sim 0.02$. In order for two nuclei to fuse, they must penetrate to a critical radius,⁸ which for the energy range considered here is $R_{\text{cr}} = r_0(A_T^{1/3} + A_P^{1/3})$, where $r_0 \approx 1.4$. In the case of ${}^9\text{Be} + {}^{28}\text{Si}$, the ${}^9\text{Be}$ has a high probability of breaking up into two α particles and a neutron, which gives rise to a large reaction cross section without particularly affecting the fusion cross sections. This picture is consistent with the elastic scattering results obtained at 45 and 60 MeV bombarding energy shown in Fig. 3, where σ/σ_C is plotted as a function of d ,¹² where

$$d = \frac{D}{A_T^{1/3} + A_P^{1/3}}$$

and

$$D = \frac{Z_T Z_P e^2}{2E_{\text{c.m.}}} \left(1 + \frac{1}{\sin \theta_{\text{c.m.}}} \right).$$

Also shown for comparison are heavy-ion ${}^{28}\text{Si}$ scattering elastic cross sections² at various energies and the ${}^{28}\text{Si} + {}^{208}\text{Pb}$ elastic scattering cross section measured at $E_{\text{c.m.}} = 145$ MeV. In order to avoid confusion, the cross section data for these latter cases are shown by solid lines, as they all lie on the same curve (CNO curve) for the case of ${}^{12}\text{C}$, ${}^{14}\text{N}$, ${}^{16}\text{O}$, and ${}^{18}\text{O}$ projectiles at the energies reported here. For large distances of closest approach (i.e., large d) the ${}^{28}\text{Si} + {}^{208}\text{Pb}$ cross section falls below the CNO curve, but then merges with it again at smaller values of d . The difference at large d in the ${}^{28}\text{Si} + {}^{208}\text{Pb}$ cross section is due to a strong reduction in the elastic scattering cross section due to the strong long-range Coulomb excitation of the 1.78 MeV state in ${}^{28}\text{Si}$. The ${}^9\text{Be} + {}^{28}\text{Si}$ elastic scattering cross sections at 45 and 60 MeV lie considerably lower than both the CNO curve and the ${}^{28}\text{Si} + {}^{208}\text{Pb}$ curve at large d . This discrepancy cannot be explained by Coulomb excitation, but is most likely due to the fact that ${}^9\text{Be}$ is loosely bound and has a large spatial extent; thereby direct reactions cause the ${}^9\text{Be}$ to break up even at large separation distances.¹³ Indeed, the reaction radius parameter calculated above, $r_R = 2.4-2.6$, is consistent with what one would estimate from inspection of Fig.

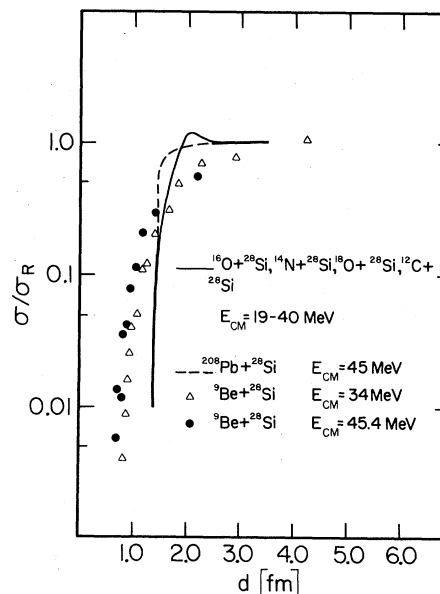


FIG. 3. Plot of σ/σ_C as a function of the reduced distance of closest approach, d , for ${}^9\text{Be} + {}^{28}\text{Si}$ at $E_{{}^9\text{Be}} = 60$ MeV (solid dots), and at $E_{{}^9\text{Be}} = 45$ MeV (open triangles). The dashed curve is σ/σ_C for ${}^{208}\text{Pb} + {}^{28}\text{Si}$ at $E_{{}^{28}\text{Si}} = 165$ MeV, and the solid curve is σ/σ_C for assorted heavy ions ($A \geq 12$) incident on ${}^{28}\text{Si}$ targets plotted as a function of d .

3. (i.e., for ${}^9\text{Be} + {}^{28}\text{Si}$ scattering at $r_R = d \approx 2.5$, reactions are taking place causing a decrease in σ/σ_R from 1). For the case of ${}^{12}\text{C} + {}^{28}\text{Si}$ and ${}^{16}\text{O} + {}^{28}\text{Si}$, the much stronger binding of ${}^{12}\text{C}$ and ${}^{16}\text{O}$ prevents any substantial breakup, and the fall from Rutherford does not occur until the nuclei are within the critical distance for fusion. It is postulated, therefore, that one of the essential differences between the heavy-ion ($A \geq 12$) scattering and the ${}^9\text{Be}$ scattering from ${}^{28}\text{Si}$ is due to the fact that the main reaction channel for the heavy-ion interactions is compound nucleus formation (i.e., fusion) which is well localized, while for ${}^9\text{Be}$ interactions it is the direct breakup of the projectile by the strong nuclear and Coulomb fields at large separation distances before fusion can occur. The fact that the calculated double folding potential for ${}^9\text{Be} + {}^{28}\text{Si}$ must be reduced by a factor of 0.4 in order to fit the measured cross sections may be related to a strong coupling between elastic and breakup channels.⁴

In summary, the fusion cross sections for ${}^9\text{Be} + {}^{28}\text{Si}$ have been measured in the range $E({}^9\text{Be}) = 30\text{--}60$ MeV. The fusion cross sections are considerably lower than the total reaction cross section over the whole energy range, while for systems which have similar compound nuclei such as ${}^{16}\text{O} + {}^{24}\text{Mg}$, ${}^{16}\text{O} + {}^{27}\text{Al}$, ${}^{12}\text{C} + {}^{24}\text{Mg}$, ${}^{12}\text{C} + {}^{27}\text{Al}$, $\sigma_{\text{FUS}} \approx \sigma_R$ at the lowest energies. These differences can be qualitatively reconciled with each other and with the anomalous elastic scattering results for ${}^9\text{Be} + {}^{28}\text{Si}$ by assuming that there is a large possibility for ${}^9\text{Be}$ breakup at large ${}^9\text{Be}$ and ${}^{28}\text{Si}$ separation distances. The ${}^9\text{Be} + {}^{28}\text{Si}$ system is an interesting one to study, as apparently the nuclear structure of ${}^9\text{Be}$ is important in determining the details of the fusion reaction and elastic scattering cross sections, even at low energies.

This work was supported in part by the U. S. National Science Foundation under the U. S.-Australia Cooperative Science Program.

¹R. Balzer, M. Hugi, B. Kamys, J. Lang, R. Miller, E. Ungricht, and J. Untermahrer, Nucl. Phys. A293, 518 (1977).

²J. S. Eck, T. R. Ophel, P. D. Clark, and D. C. Weissner, Nucl. Phys. A334, 519 (1980).

³M. S. Zisman, J. G. Cramer, R. M. DeVries, D. A. Goldberg, and J. W. Watson, *1977-1978 Nuclear Science Annual Report of the Lawrence Berkeley Laboratory*, edited by L. S. Schroeder, R. A. Gough, and M. J. Nurmia (Lawrence Berkeley Laboratory, Berkeley, 1978), p. 72.

⁴G. R. Satchler, Phys. Lett. 83B, 284 (1979).

⁵G. R. Satchler and W. G. Love, Phys. Rep. (to be published).

⁶G. R. Satchler and W. G. Love, Phys. Lett. 65B, 415 (1976).

⁷R. Bass, Nucl. Phys. A231, 45 (1974).

⁸D. Glas and U. Mosel, Nucl. Phys. A237, 429 (1975).

⁹M. M. Fowler and R. C. Jared, Nucl. Instrum. Methods 124, 341 (1975).

¹⁰G. F. Geesaman, C. N. Davids, W. Henning, D. G. Kovar, K. E. Rehm, J. P. Schiffer, S. L. Tabor, and F. W. Prosser, Phys. Rev. C 18, 284 (1978).

¹¹D. G. Kovar, G. F. Geesaman, T. H. Braid, Y. Eisen, W. Henning, T. R. Ophel, M. Paul, K. E. Rehm, S. J. Sanders, P. Sperr, J. P. Schiffer, S. L. Tabor, S. Vigdor, B. Zeidman, and F. W. Prosser, Phys. Rev. C 20, 2147 (1979).

¹²P. R. Christensen, V. I. Manko, F. D. Becchetti, and R. J. Nickles, Nucl. Phys. A207, 33 (1973).

¹³J. Untermahrer, J. Lang, and R. Muller, Phys. Rev. Lett. 40, 1077 (1978).